

Springs is located near the entrance of the wind corridor, making it more susceptible to the synoptic events that occur in the winter. Since Laramie is located at the exit of the wind corridor, the winds must be reasonably strong to get through the wind corridor. Cheyenne, located to the east of the Laramie Range, only experiences the synoptic events producing winds which blow through the wind corridor and then around or over the Laramie Range. These additional topographic constraints do not apply at Rock Springs and as such, the synoptic modes have a much greater impact.

These results confirm that the atmospheric reasoning behind the behavior of the wind resource is sound: the winter time is dominated by a synoptic mode. Per the discussion in Chapter 4, as the jet stream travels south in the winter, areas of low and high pressure form to the east and west of Wyoming, resulting in a strong pressure gradient across the state. The frequency of the jet stream is, on average, on the order of a week to ten days. Conversely, during the summer time when the jet stream has retreated northward, the synoptic mode is all but gone from the summertime FFT plots; and thus the wind resource is weaker during the summer months.

5.2: Probability Distribution Analysis

The persistence of the wind, up to now, has been taken on merit and a few maps with rated velocities. A PDF is a statistical tool that can help verify the persistence of the wind in the southeastern corner of Wyoming. All the 10-m wind speeds during winter of 2009 were extracted from the North American Model (NAM) 12-km output at a representative point,

denoted by the burgundy asterisk in Figure 5.4. The darkened black area corresponds to the white areas of Class 7 wind resource in the maps in Chapter 4.

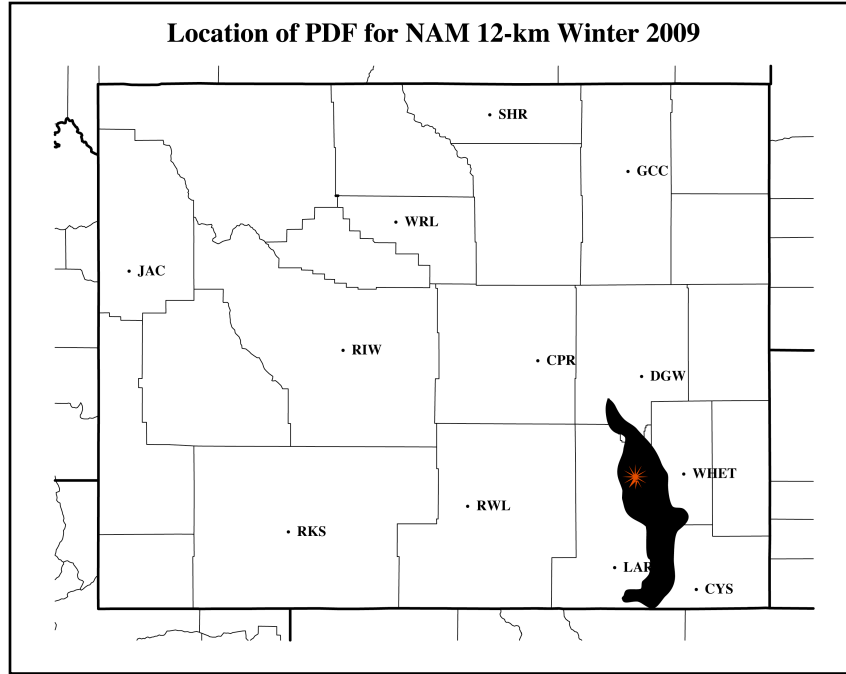


Figure 5.5: Location where NAM 12-km winter 2009 data was extracted for probability analysis. The filled in black area denotes Class 7 wind resource.

The data were binned in increments of 1.5 m s^{-1} from 0 to 21 m s^{-1} . The first bin, for example, contains all wind speeds between 0 and 1.5 m s^{-1} , the second bin contains all wind speeds from 1.5 m s^{-1} to 3 m s^{-1} , *etc.* The probabilities were all calculated by Equation 3.8. A Weibull curve, as outlined by Equation 3.9 was also calculated. The PDF can be seen in Figure 5.6. The horizontal axis labels correspond to the middle value of each bin. The first bin contains wind speeds for 0 to 1.5 m s^{-1} and the midpoint is 0.75. The shape parameter (k) and the scale parameter (c) of the Weibull curve, the standard deviation (ϕ) and the mean (\bar{u}) are outlined in Table 5.1. The shape and scale parameters were calculated per Equations 3.10 and 3.11.

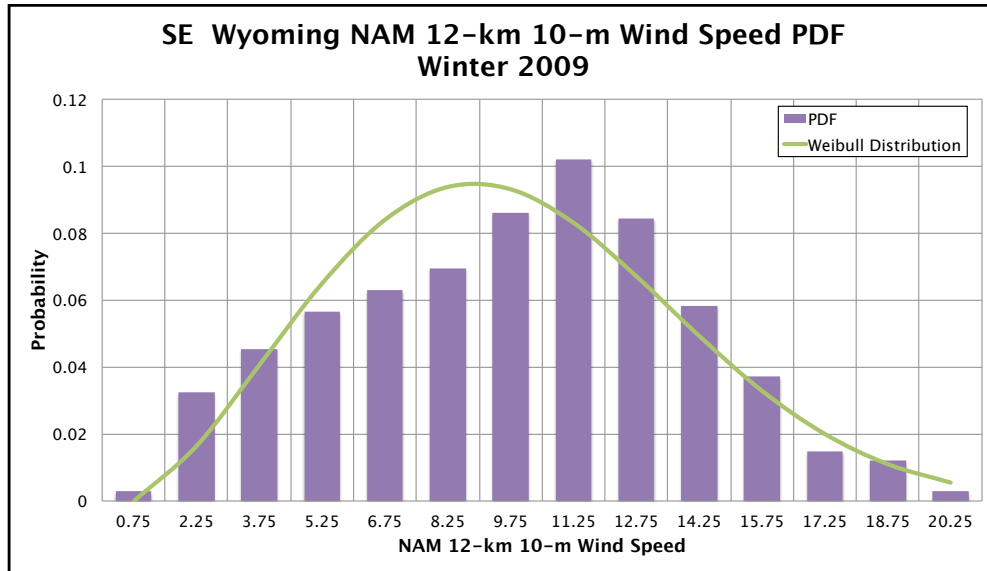


Figure 5.6: PDF of the NAM 12-km winter 2009 data in southeastern Wyoming. The green line denotes the calculated Weibull fit.

Table 5.1: Statistical and fit parameters for the Weibull curve in Figure 5.6.

Parameter	Value
k	2.38
c	10.23-m s ⁻¹
ϕ	4.09-m s ⁻¹
\bar{u}	9.07-m s ⁻¹

This is exactly the type of PDF one would hope to see in a windy area. The highest probability, which can be taken as a proxy for the average, is the bin of wind speeds between 10.5 m s⁻¹ and 12 m s⁻¹. For reference, the maximum average 10-m wind speed for Class 7 wind resource is 9.4 m s⁻¹. The most common wind speeds at this location are beyond the specifications for Class 7 wind proving that the winds in this area are persistently strong.

Though this PDF nicely illustrates the regularity of the winds, the PDF reflects NAM 12-km data. The location chosen is also atop the Laramie Range, an unlikely site for a wind farm. More useful would be PDFs at places where model data can be corroborated with observational data. PDFs for summer and winter 2008-2010 at three sites: Laramie, Cheyenne and Rock Springs and three year averages are shown on the following pages. Red bars represent summer and blue bars represent winter. Lighter reds and blues are for the observational data and darker reds and blues are for the NAM 12-km. Each plot also has a Weibull distribution fitted to it, plotted in green. The vertical scale for the plots of the individual years are different than those in the three year average plots. Table 5.2 summarizes the averages, standard deviations and Weibull fit parameters for 2008-2010 plus the three year averages for each site. The three hourly data were binned in 1.5 m s^{-1} increments according to the seasonal divisions outlined in Table 3.4. The horizontal labels, as in Figure 5.6, reflect the midpoint of each division.

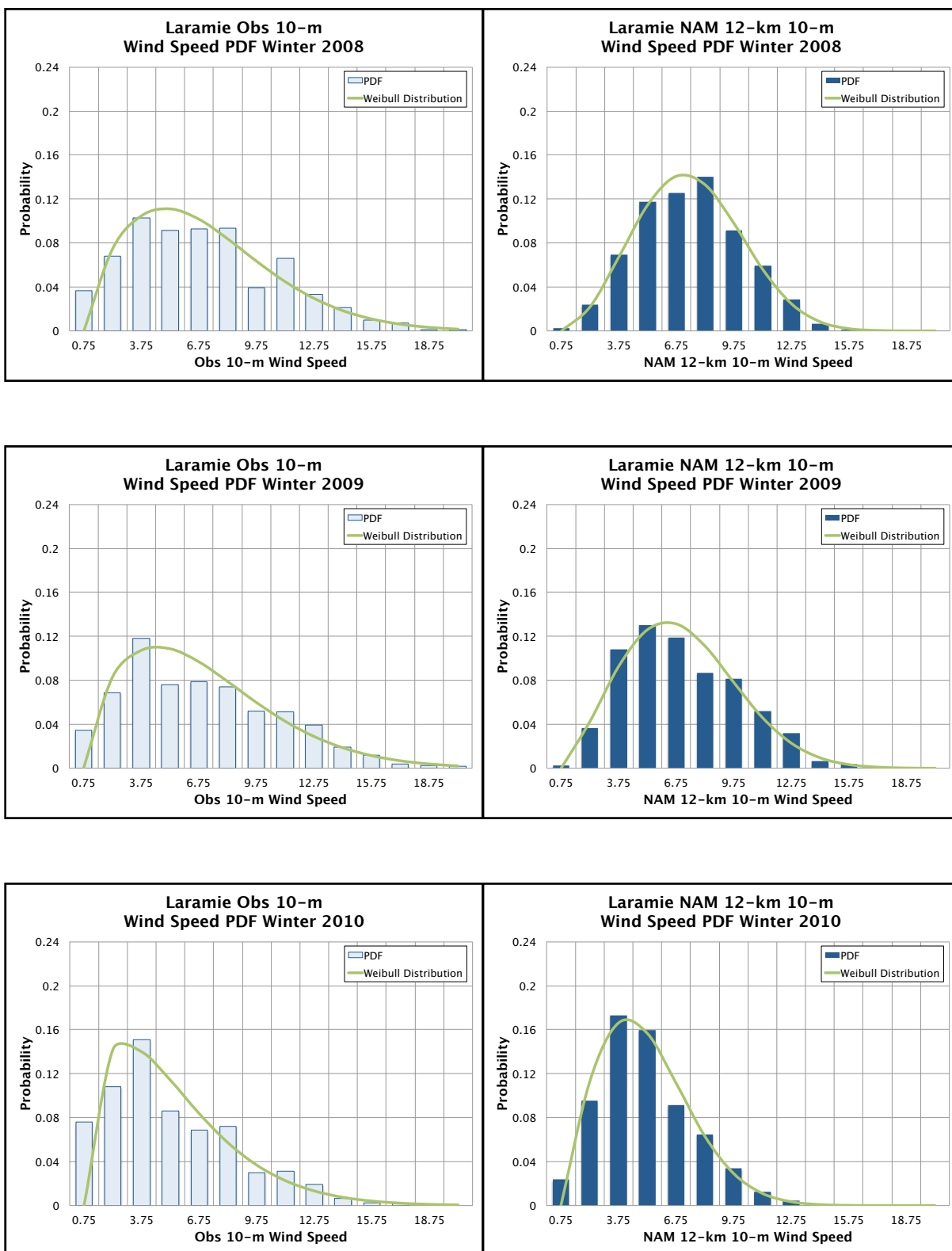


Figure 5.7: Laramie observations (Obs) and NAM 12-km PDF winter 2008-2010.

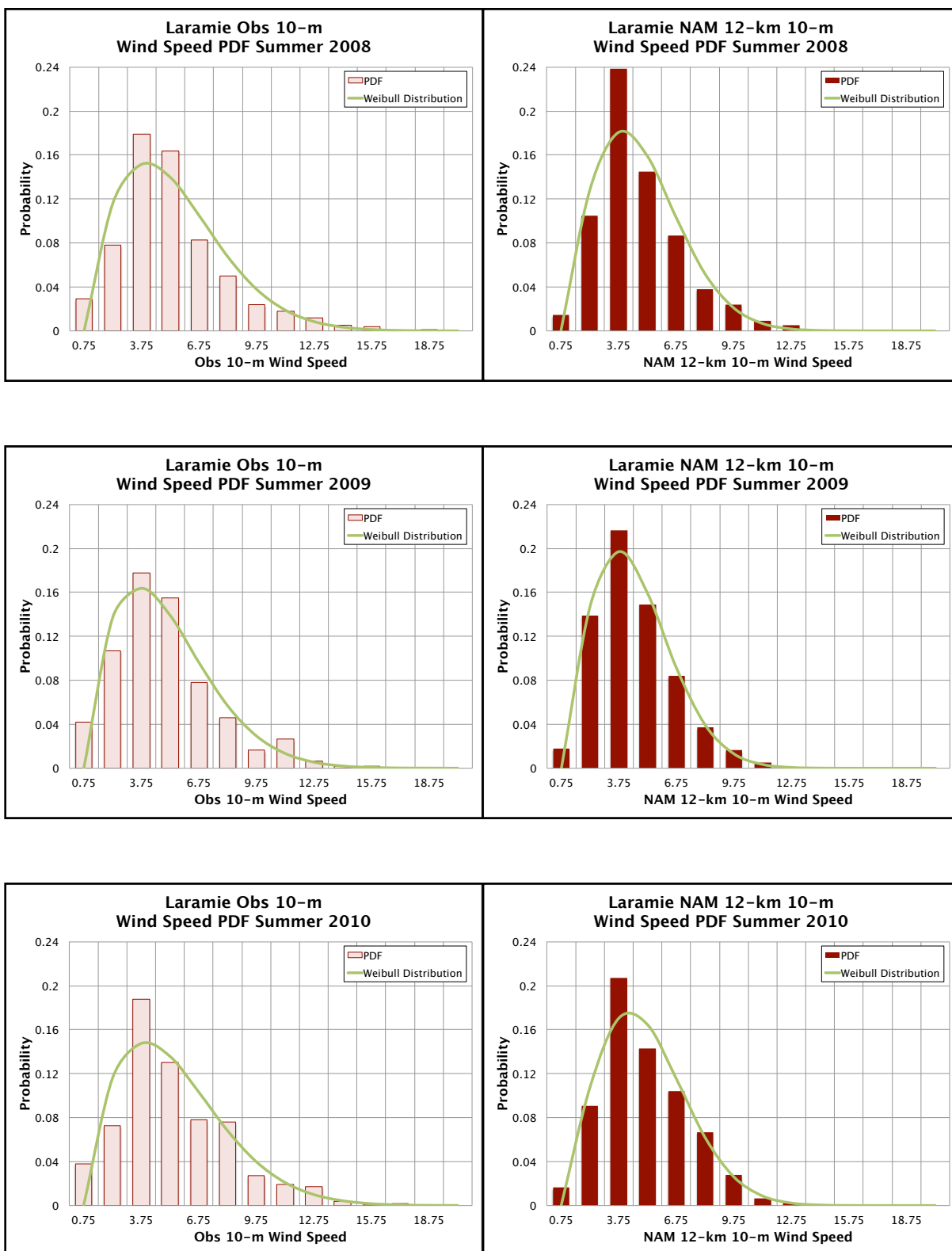


Figure 5.8: Laramie observations (obs) and NAM 12-km PDF summer 2008-2010.

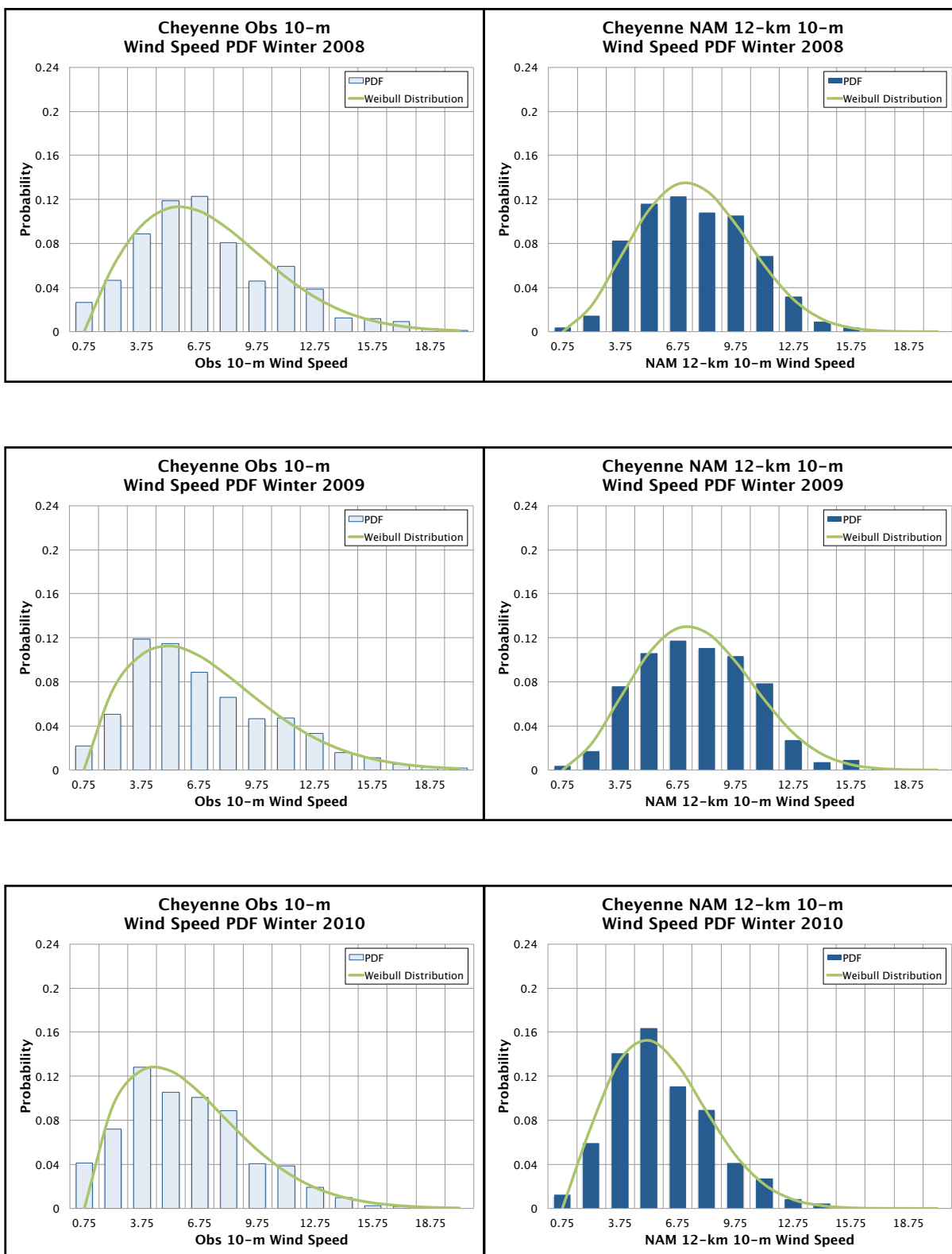


Figure 5.9: Cheyenne observations (obs) and NAM 12-km PDF winter 2008-2010.

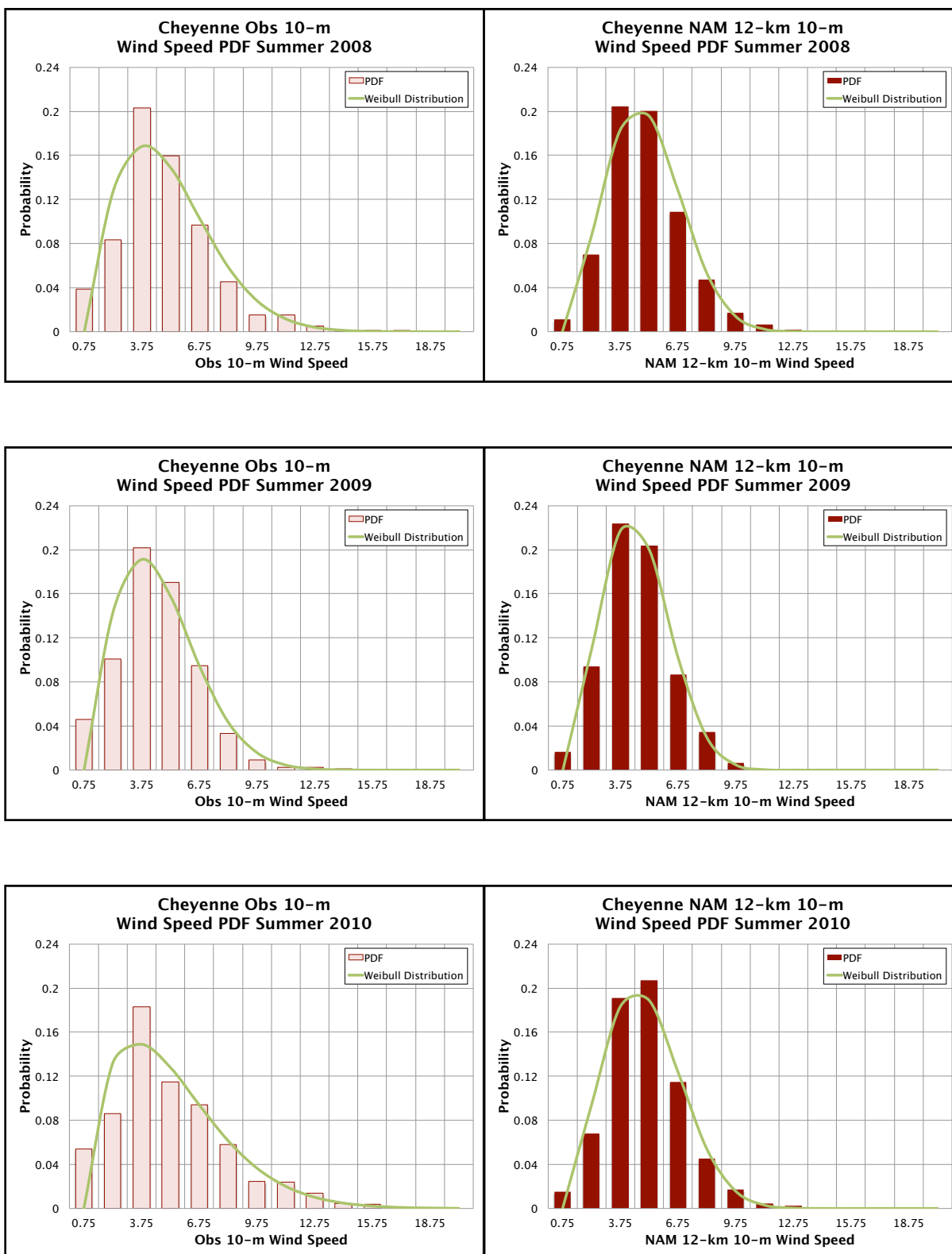


Figure 5.10: Cheyenne observations (obs) and NAM 12-km PDF summer 2008-2010.

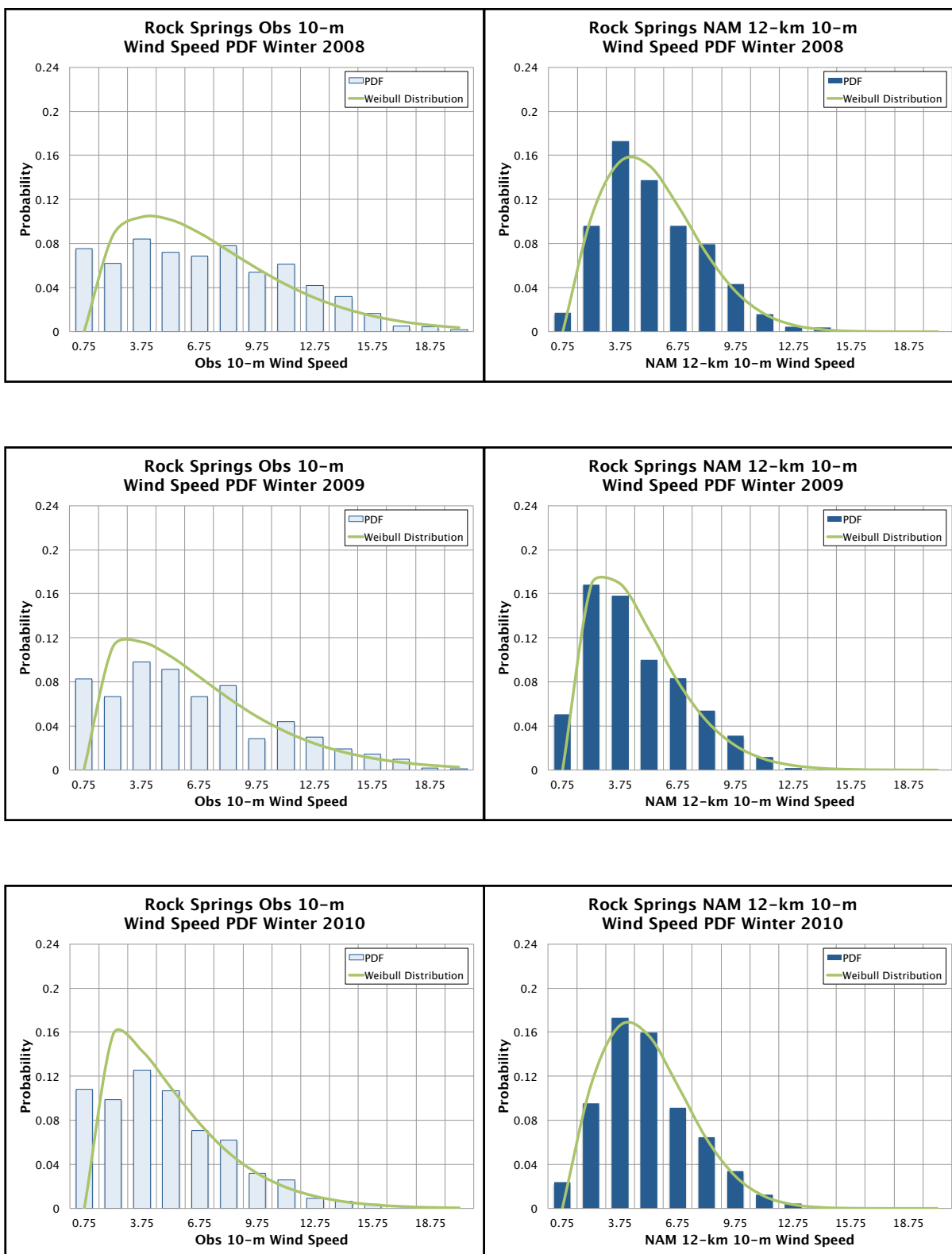


Figure 5.11: Rock Springs observations (obs) and NAM 12-km PDF winter 2008-2010.

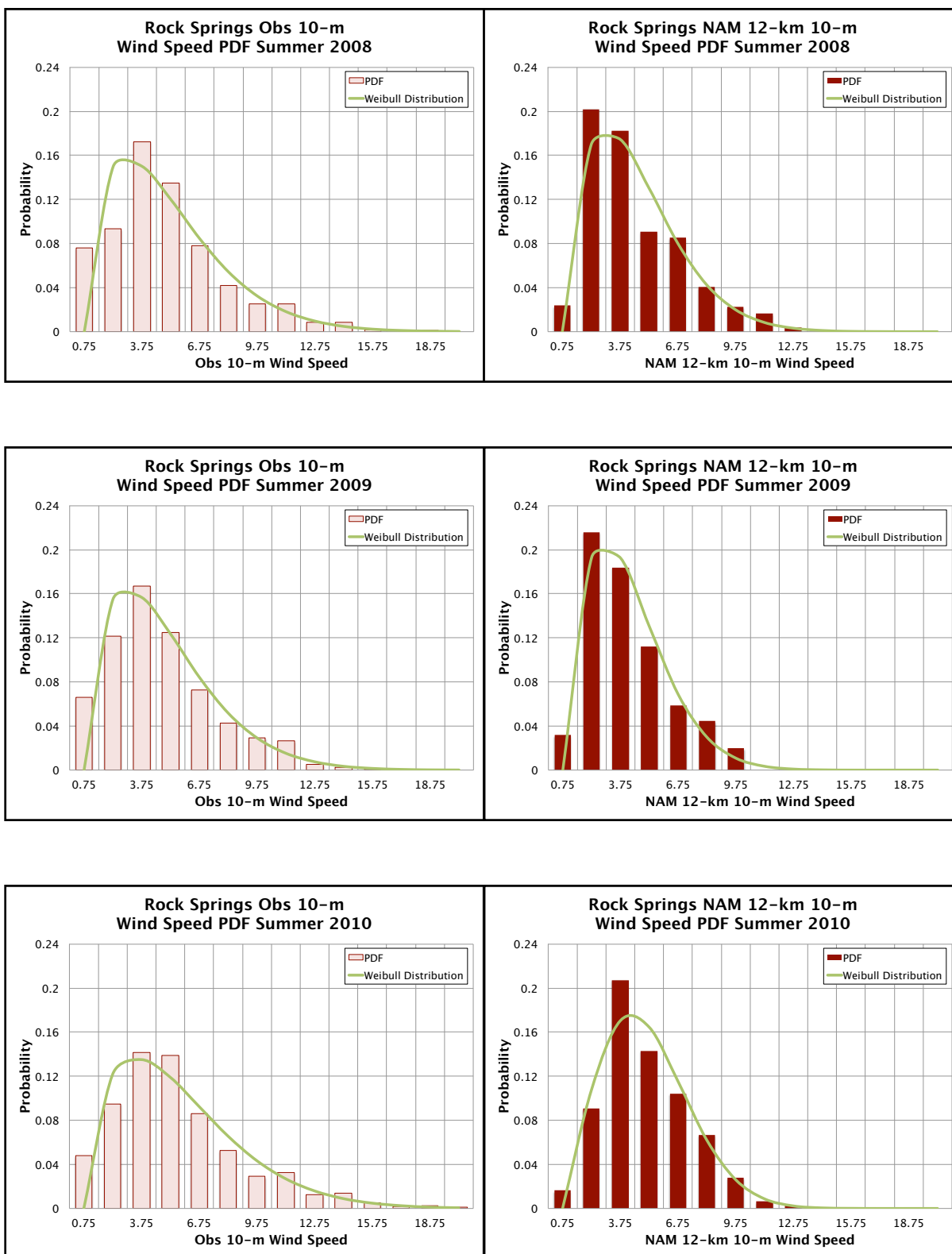


Figure 5.12: Rock Springs observations (obs) and NAM 12-km PDF summer 2008-2010.

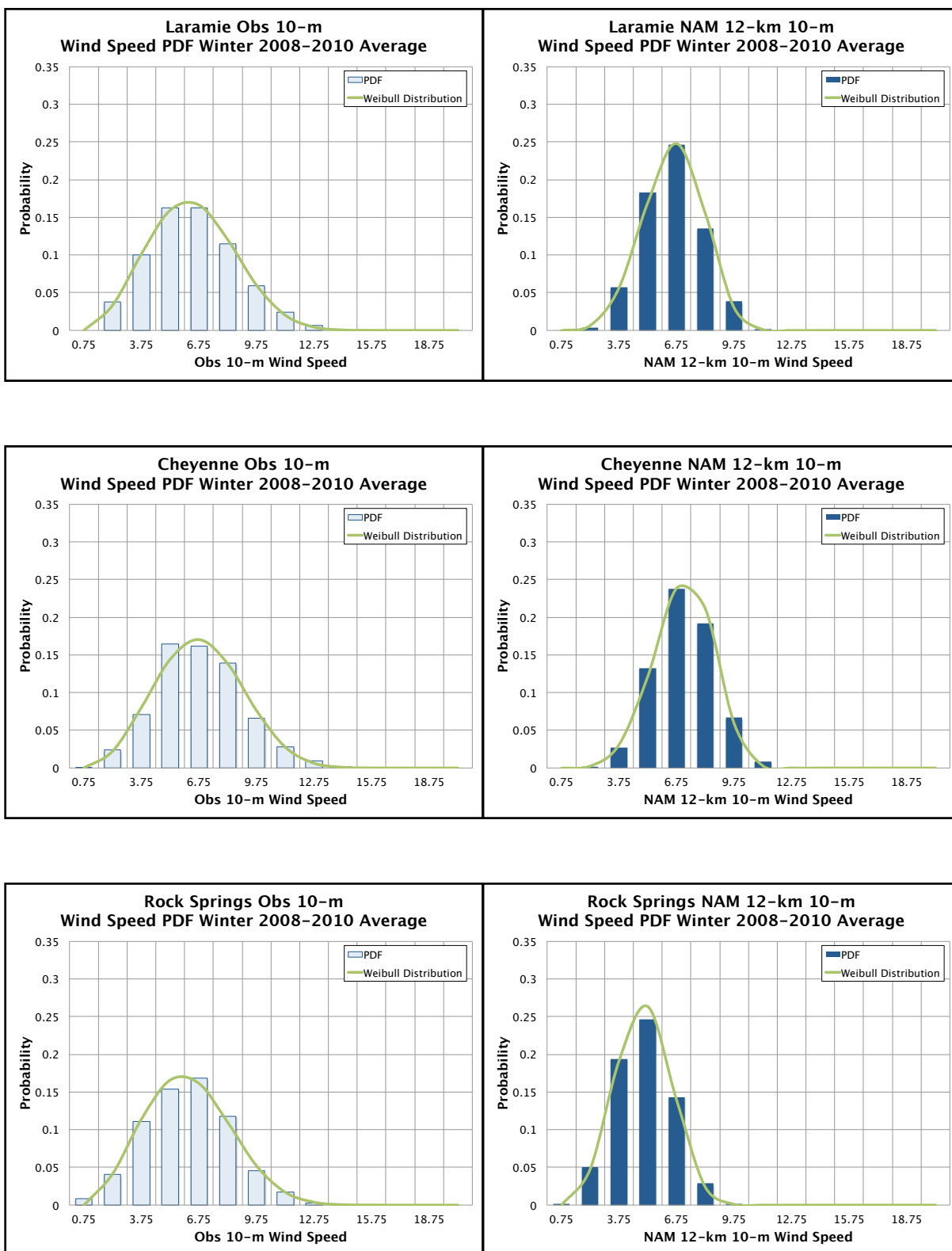


Figure 5.13: winter three year averages of observations (obs) and NAM 12-km for LAR, CYS and RKS. Note the vertical scale has increased to 0.35.

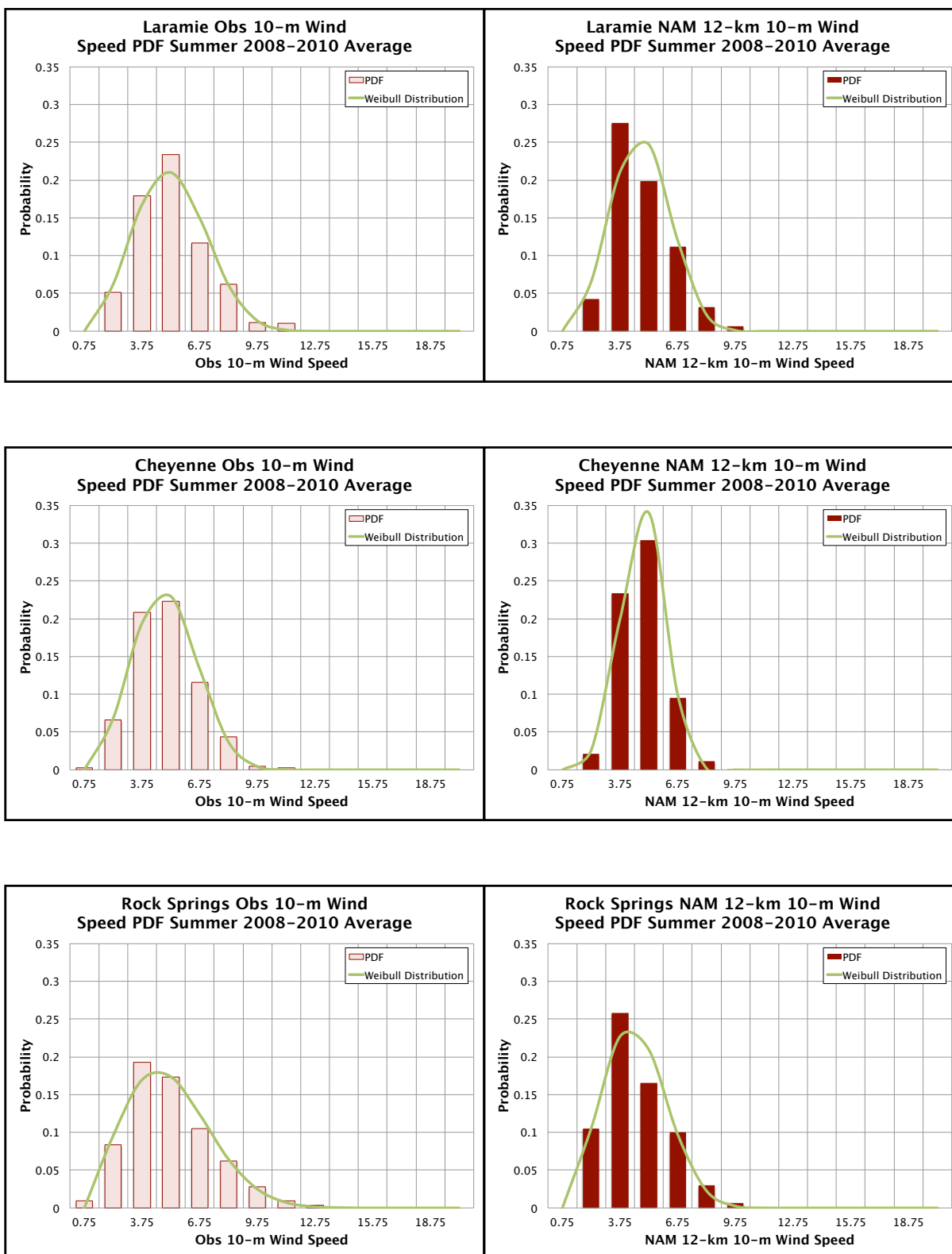


Figure 5.14: summer three year averages of observations (obs) and NAM 12-km for LAR, CYS and RKS. Note the vertical scale has increased to 0.35.

The overall shape of the PDFs and Weibull curves speaks to the variability of the resource. The shape parameter, k , dictates the width of the Weibull curve: higher values of k correlate to narrower curves. Narrower curves imply the data is more concentrated, resulting in a smaller standard deviation. Table 5.2 verifies this general relationship: the Cheyenne summer 2009 model plot, for example, is quite narrow with a k value of 2.45 and a standard deviation of 1.70 m s^{-1} . Wider curves exhibit higher standard deviations suggesting more variability. During both winter and summer, but especially in the winter, the observational plots have much more spread than their modeled counterparts. These fluctuations present, at best, a challenge to simulate. The yearly model plots seem to be more symmetric about the peak of the PDF value than the observational plots and the three year average plots of both modeled and observed datasets display the greatest degree of symmetry.

Comparing the shape and magnitude of the model and observational PDFs, the summertime claims the greatest similarity. Both sets of PDFs are consistent with lower wind speeds, which, as has been demonstrated, are more prevalent in the summer. In some cases, *e.g.* Rock Springs 2010 and Laramie 2008, lower model bins peak much higher than the fitted Weibull curves and all of the observational bins. One limitation of the model is that it can never simulate a 0 m s^{-1} wind-- all model output wind speeds are always greater than zero. Because higher wind speeds result in higher wind power densities (WPDs), this shortcoming of the model is usually neglected. The model's bias towards weaker nonzero wind speeds is the culprit for these anomalously high bins. The trailing edge of both the Weibull curve and the PDF is longer for the observational plots than the model plots. Since the lower wind speeds dominate in the summertime, this discrepancy becomes less of an issue. However,

when lower wind speeds are less common, these high wind speed bins significantly impact the details of the WPD landscape.

The differences between the model and observations become much more apparent in the wintertime. In general, the maxima of the model plots are higher than the observational maxima. Higher PDF peaks imply lower standard deviation meaning that the variability of the model is not representative of the observational variability. The model plots also exhibit more symmetry, indicating an equal chance of high or low wind speeds. Conversely, the observational plots are skewed to the left, indicating a higher probability of low wind speeds, consistent with the lower model WPD observed in Chapters 4 and 5. The trailing edge of the Weibull curve for the observational plots extends farther to the right compared to the model. At 10 m, a 1.5 m s^{-1} change can be the difference of two wind classes. Even though the probability of these higher wind speeds is low on the observational plots, the fact that they are absent in the model plots compromises the model's ability to accurately predict WPD. Rock Springs 2008 serves as an excellent example of this. The NAM 12-km curve posits winds 3 to 4.5 m s^{-1} occur with the highest probability. The observational plot reports roughly equal probabilities of wind from 0 to 10.5 m s^{-1} . These discrepancies underline the biases toward weaker, more organized wind speeds in the model.

The three year average PDFs, more climatologically stable and arguably more representative of the winds at these locations, further illustrate the shortcomings in the model. In every summer and winter plot, the model peak is higher and narrower than the observational plot. Table 5.2 also confirms that the three year standard deviations of the model at all three locations for both seasons is lower than the observational standard

deviations. These three year single values of average wind speed and standard deviation, however, must be interpreted within the appropriate context. Only looking at the average three year wind speeds in Table 5.2 for each season masks many of the characteristics of the resource. In the winter, the average three year model wind speed for Laramie and Cheyenne is larger than the three year average of the observed wind speeds. Armed with only this information, one would conclude that the model over-predicts the wind and thus the WPD. The comparisons in Chapter 4 show that is not the case. The standard deviations, which can be taken as an indicator of the variability of the resource, reveal the observational data has much more variability, or spread, than their modeled counterparts. Knowing that the model under-predicts strong winds and over-predicts weaker winds helps explain the narrowness of the model plots. The agreement between the PDFs and the fitted Weibull curves in these plots further justifies modeling the resource with the Weibull function.

This behavioral difference between the model and observation may be partly responsible for the model's poor performance. Unfortunately, the solution is not as simple as "making the model more random," as simulating randomness is limited with current NWP models. These plots do however emphasize the need for more realistic simulations. Since the model is able to capture the longer term trends in the resource (diurnal and seasonal), simulating short-term ramp events are probably the model's largest handicap.

5.3: Validity of the 1/7 Power Law

Not much has been said about the validity of the 1/7 Power Law, the method used by the wind industry and in all the maps in Chapter 3 to calculate the wind at 50 m. The

Cooperative Surface-Atmosphere Exchange study field campaign of October 1999 (CASES-99) was a month long investigation of the nocturnal boundary layer. Data was recorded on a tower in 10-m increments from 10 m to 50 m at a sample rate of 5 minutes (Banta et al. 2002). Figure 5.14 shows the results for the first five days. The left vertical axis references the recorded 50-m wind speed and the extrapolated 50-m wind speed via the $1/7$ Power Law (Equation 3.1). The right vertical axis references the contour number, n , in the $1/7$ Power Law. The green and black lines correspond to sunset and sunrise, respectively. The pink line represents the value of $1/7$ and the olive yellow line is the calculated contour number based on the wind at 50 m and the wind at 10 m.

Several trends become apparent just within the first few days. The second and third days are windiest, illustrating the diurnal variability of the resource. The winds tend to increase between sunset and sunrise: after day three is a prime example of this. Most relevant, however, are the discrepancies between the actual 50-m wind and the extrapolated 50-m wind via the $1/7$ Power Law. During the day, the two lines shadow each other quite well, *e.g.* days two and four. When the two lines are in agreement, the contour line (olive yellow) is nearly atop the $1/7$ line (pink). During the night, though, the two lines diverge substantially. The extrapolated winds are always lower than the actual winds and the corresponding contour number is greater than $1/7$. Physically this makes sense. The $1/7$ Power Law is designed to calculate upper level winds based on lower level winds. During the day, when the boundary layer is turbulent and well mixed, there is a stronger link between the 10-m wind and the 50-m wind. Thus the $1/7$ Power Law accurately predicts winds at 50 m based on winds at 10 m. At nighttime, the boundary layer becomes stratified and much less